# A Single Synchronous Controller for High Penetration of Renewable Energy Resources into the Power Grid

Majid Mehrasa
C-MAST/UBI, Covilha, Portugal
m.majidmehrasa@gmail.com

Edris Pouresmaeil
Dep. of Elec. Eng. and Auto. Aalto University, Finland
edris.pouresmaeil@gmail.com

Mousa Marzband
Dep. of Mech. and Elec. Eng., Northumbria University, UK
mousa.marzband@northumbria.ac.uk

João P. S. Catalão
INESC TEC and FEUP, Porto, C-MAST/UBI, Covilha, and INESC-ID/ IST-UL, Lisbon, Portugal
catalao@fe.up.pt

***Abstract*—A single synchronous controller (SSC) technique is proposed in this paper for control of interfaced converters under high penetration of renewable energy resources (RER) into the power grid. The proposed SSC is based on a new dynamic model concerning to the power grid stability (PGS) and modeled based on all features of a synchronous generator (SG), which can properly improve the performance of the power grid in those scenarios in which a large-scale penetration of RERs is considered. Different transfer functions are achieved to assess the high performance of the proposed control technique. Simulation results are presented to demonstrate the superiority of the proposed SSC in the control of the power electronic-based synchronous generator under high penetration of RERs into the power grid.**

***Keywords—Single synchronous controller (SSC), Low-value inertia, Virtual mechanical power (VMP), Virtual angular frequency (VAF), Renewable energy resources (RERs).***

## I. Introduction

The important roles of distributed generation technology especially based on renewable energy resources (RERs) in power system [1]-[3] and different concerns associated to the instable operation of power grid under high penetration of RERs have been studied highly in the literature in recent years.

In some studies authors focused on using distributed energy storage systems (DESSs) for encountering such stability problems counter them through the design of an optimized supervisory and advanced controllers for large-scale DESSs with the aim of reliable and stable integration of RERs with the power grid [4]-[6].

In other studies in order to compensate the voltage rise of the power grid caused by the excess of PV sources, the reactive power based controllers proposed for the interfaced converters in DG units [7]-[9].

In this paper, a single synchronous controller (SSC) is proposed based on an active and reactive power-based dynamic model with the aim of providing a stable operation for the power grid under high penetration of RERs.

J.P.S. Catalão acknowledges the support by FEDER funds through COMPETE 2020 and by Portuguese funds through FCT, under Projects SAICT-PAC/0004/2015 - POCI-01-0145-FEDER-016434, POCI-01-0145-FEDER-006961, UID/EEA/50014/2013, UID/CEC/50021/2013, UID/EMS/00151/2013, 02/SAICT/2017 - POCI-01-0145-FEDER-029803, and also funding from the EU 7th Framework Programme FP7/2007-2013 under GA no. 309048.

The rest of this paper is organized as follows. Achieving the proposed active and reactive power based dynamic model is presented in the first subsection of Section II. Then, the Section II is completed by designing the proposed SSC. Two transfer functions are obtained in Section III to assess the effects of different parameters related to the SSC on the ability of the SSC at presenting accurate active and reactive power sharing as well as power grid stability (PGS). Finally, simulation results are given in Section IV and conclusions are drawn in Section V.

## II. Proposed Model

The general model based on the interfaced-converter for integration of large-scale RERs is drawn in Fig. 1. This figure contains the power grid, loads, permanent magnet synchronous generator (PMSG), two types of controllable RER, and grid-feeding RERs which will be discussed further in the subsequent sections.

### A. The Mathematical Model Description

The dynamic model of the proposed model in Fig. 1 should be extracted in order to draw a control technique for control of the interfaced converter for integration of large-scale RERs into the power grid.

By this assumption, the dynamic equations of the proposed model in *dq* reference frame can be expressed as [10]:

$$L\frac{di_d}{dt} + Ri_d - \omega Li_q - u_d v_{dc} + v_d = 0 \quad (1)$$

$$L\frac{di_q}{dt} + Ri_q + \omega Li_d - u_q v_{dc} + v_q = 0 \quad (2)$$

$$C\frac{dv_{dc}}{dt} + u_d i_d + u_q i_q + i_{dc} = 0 \quad (3)$$

The instantaneous active and reactive power of RER-based interfaced converter (REIC) can be stated as $P=i_d v_d$ and $Q=-i_q v_d$. By neglecting the partial variations, a set of new active and reactive power based dynamic equations can be obtained through multiplying the d-component of the reference voltage ($v_d$) to (1)-(3).

978-1-5386-5186-5/18/$31.00 ©2018 IEEE

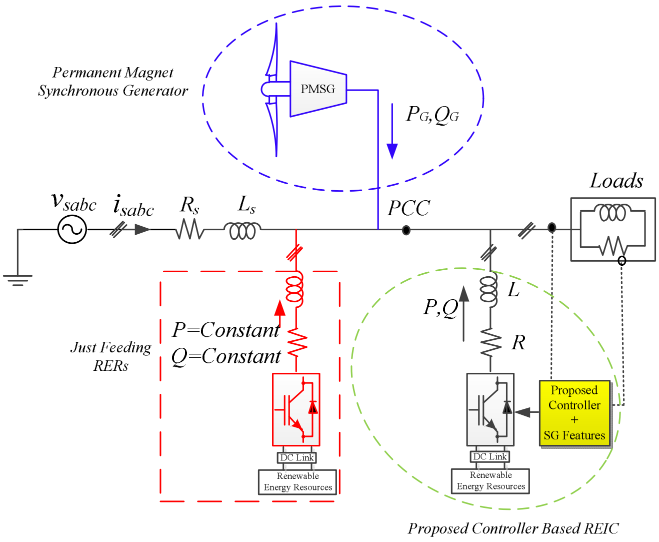


Fig. 1. SSC-based converter model along with the power grid.

$$\frac{L}{R}\frac{dP}{dt}+P+\frac{\omega L}{R}Q-u_dP_{c1}+P_d=0 \tag{4}$$

$$\frac{L}{R}\frac{dQ}{dt}+Q-\frac{\omega L}{R}P+u_qP_{c1}-P_{dq}=0 \tag{5}$$

$$RC\frac{dP_{c1}}{dt}+u_dP-u_qQ+P_{c2}=0 \tag{6}$$

where, $P_{c1}=v_{dc}v_d/R$, $P_{c2}=i_{dc}v_d$, $P_d=v_d^2/R$, and $P_{dq}=v_dv_q/R$.

### *B. Presentation of the Proposed Single Synchronous Controller (SSC)*

In this section, the proposed single synchronous controller (SSC) technique is discussed in detail. As intended, the proposed controller should follow the inherent features of SG. Then, the proposed dynamic model along with the combination of these features is used to design the final controller for the control of the interfaced converter. The following subsections elucidate the designing process.

#### *B.1. The SG Characteristics Extraction*

The main concerns associated with high penetration of RERs are the unstable behaviors of the voltage magnitude and the frequency of the power grid due to odd transient dynamics of interfaced converters and the lack of inertia of this kind of generators [11]. These concerns can be noticeably decreased by considering all the properties of synchronous generators in the structure of the control loop of interfaced converter. As it is known, the swing equation of a SG can be stated as:

$$J\frac{d\omega}{dt}=\frac{P_m-P}{\omega} \tag{7}$$

where, $J$, $\omega$, $P$, and $P_m$ are moment inertia, angular frequency, electrical power, and mechanical power of SG respectively. Using the small-signal linearization for (7) and performing some simplifications, (8) can be achieved as:

$$\Delta\omega=\frac{1}{\omega^*J}\cdot\frac{\Delta P_m-\Delta P}{s+\left(P_m^*-P^*\right)/\omega^{*2}J} \tag{8}$$

Considering (8), the active power variation can be written based on variations of the virtual mechanical power and virtual angular frequency as:

$$\frac{\Delta P}{s}=\frac{\Delta P_m}{s}-\left(\omega^*J+\frac{\left(P_m^*-P^*\right)}{\omega^*s}\right)\Delta\omega \tag{9}$$

Equations (8) and (9) can lead to constructing an important part of the ultimate controller consisted of all properties of SG as shown in Fig. 2. As it is depicted, the error parts of VMP and VAF are utilized for the active power-axis of the SSC. Moreover, the scenario used for achieving the virtual angular frequency can be employed for both active and reactive-axis of the proposed SSC.

By considering a low pass filter (LPF) as $\omega_1/(s+\omega_2)$ , LPF coefficients and the coefficients of PI controller associated with virtual angular frequency error can be driven as:

$$\omega_1=\frac{1}{\omega^*J},\omega_2=\left(P_m^*-P^*\right)/\omega^{*2}J \tag{10}$$

$$k_{p\omega}=\omega^*J,\ \ k_{i\omega}=\left(P_m^*-P^*\right)/\omega^* \tag{11}$$

$$k_{pp}=1/\omega^*J,\ \ k_{ip}=\left(P_m^*-P^*\right)/\left(\omega^{*3}J^2\right) \tag{12}$$

It can be understood from (10) and (11) that all coefficients are highly dependent on inertia, reference values of active power, VMP, and VAF.

#### *B.2. The Proposed Controller*

According to Fig. 2, the active and reactive axis of the proposed control technique can be written as:

$$u_d=\frac{1}{P_{c1}}\left(\begin{array}{l}\left(\Delta P-\Delta P_m\right)\left(k_{pp}+k_{ip}/s\right)+\left(\Delta\omega\right)\left(k_{p\omega}+k_{i\omega}/s\right)\\+\left(\left(\Delta P-\Delta P_m\right)\left(\dfrac{\omega_1}{s+\omega_2}\right)+\omega^*\right)\alpha\dfrac{L}{R}Q+P_d\end{array}\right) \tag{13}$$

$$u_q=\frac{-1}{P_{c1}}\left(\begin{array}{l}\Delta Q\left(k_{pq}+k_{iq}/s\right)-\\\left(\left(\Delta P-\Delta P_m\right)\left(\dfrac{\omega_1}{s+\omega_2}\right)+\omega^*\right)\beta\dfrac{L}{R}P-P_{dq}\end{array}\right) \tag{14}$$

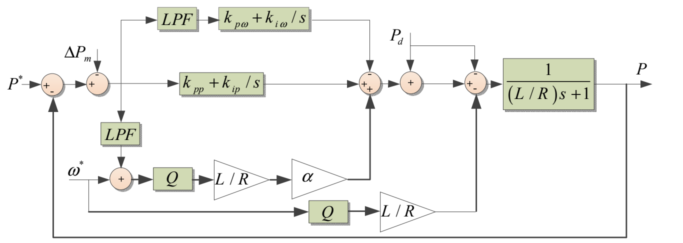


(a)

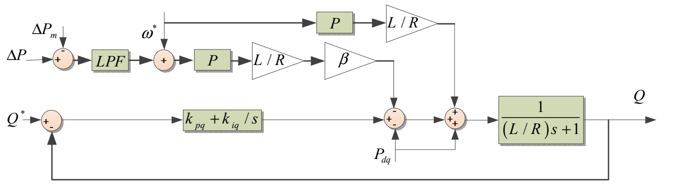


(b)

Fig. 2. The proposed single synchronous controller (SSC): (a) active power component, (b) reactive power component.

Equations (13) and (14) show that both d and q axis of the SSC are affected by the features of the SG.

This advantage can significantly cause the added inherent features of the SG to make more contributions in the operation of REIC in power grid stability under high penetration of RERs. This advantage is analyzed in the next sections.

## III. Active and Reactive Power Sharing Evaluation

As can be seen from Fig. 2, both active and reactive power and their reference values are used as output and input of closed-loop descriptions of the SSC, respectively. The coefficients of α and β are the decoupled factors of closed loop descriptions that can vary the amount of decoupled relationship between the active component of the SSC and the reactive power and vice versa.

In fact, these coefficients make relationship between P and Q in the SSC. By considering two closed-loop diagrams in Fig. 2, two transfer functions related to active and reactive power are driven as:

$$\frac{P}{P^*}=\frac{\left(\begin{array}{l}\left(\left(Lk_{pp}/R\right)s^4+\left[\left(L/R\right)\left(k_{ip}+k_{pp}\omega_2-\omega_1 k_{p\omega}\right)+\left(k_{pp}\right)\left(1+k_{pq}\right)\right]s^3\right)\\+\left[\begin{array}{l}\left(L/R\right)\left(k_{ip}\omega_2-\omega_1 k_{i\omega}\right)+\left(1+k_{pq}\right)\left(k_{ip}+k_{pp}\omega_2-\omega_1 k_{p\omega}\right)+k_{pp}k_{iq}+\\ \alpha\omega_1 k_{pq}\dfrac{L}{R}\end{array}\right]s^2\\+\left[\left(k_{ip}\omega_2-\omega_1 k_{i\omega}\right)\left(1+k_{pq}\right)+k_{iq}\left(k_{ip}+k_{pp}\omega_2-\omega_1 k_{p\omega}\right)+\alpha\omega_1 k_{iq}\left(L/R\right)\right]s\\+\left(k_{ip}\omega_2-\omega_1 k_{i\omega}\right)k_{iq}\end{array}\right)}{\left(\begin{array}{l}\left(L/R\right)^2 s^5+\left(L/R\right)\left(2+k_{pp}+\left(L/R\right)\omega_2+k_{pq}\right)s^4\\+\left(\begin{array}{l}\left(L/R\right)\left(k_{pp}\omega_2+k_{ip}-k_{p\omega}\omega_1\right)+k_{pp}\left(1+k_{pq}\right)+\\ \left(L/R\right)k_{iq}+\left(\left(L/R\right)\omega_2+1\right)\left(1+k_{pq}\right)+\left(L/R\right)\omega_2\end{array}\right)s^3\\+\left(\begin{array}{l}\left(L/R\right)\left(k_{ip}\omega_2-k_{i\omega}\omega_1\right)+\left(1+k_{pq}\right)\left(k_{pp}\omega_2+k_{ip}-k_{p\omega}\omega_1\right)\\+k_{pp}k_{iq}+\alpha\omega_1 k_{pq}\dfrac{L}{R}+\left(\left(L/R\right)\omega_2+1\right)k_{iq}+\omega_2\left(1+k_{pq}\right)\end{array}\right)s^2\\+\left(\begin{array}{l}\left(1+k_{pq}\right)\left(k_{ip}\omega_2-k_{i\omega}\omega_1\right)+k_{iq}\left(k_{pp}\omega_2+k_{ip}-k_{p\omega}\omega_1\right)\\+\alpha\omega_1 k_{iq}\left(L/R\right)+\omega_2 k_{iq}\end{array}\right)s+\left(k_{ip}\omega_2-k_{i\omega}\omega_1\right)k_{iq}\end{array}\right)} \quad (15)$$

$$\frac{Q}{Q^*}=\frac{k_{pq}s+k_{iq}}{\left(L/R\right)s^2+\left(1+k_{pq}\right)s+k_{iq}} \quad (16)$$

Equation (15) shows that the transfer function related to the active power of REIC and its reference value are highly dependent on the SG features and its related controllers. The Nyquist diagrams of $P/P^*$ for various low-value inertias are drawn in Fig. 3.

As can be seen for the smallest inertia value, the ratio of $P/P^*$ is extremely near to 1 around the reference of the angular frequency that confirms the accurate active power tracking of the proposed SSC in this condition.

Also, the aforementioned explanation is true for $J_2$ with slightly less accuracy. Instead, for $J_3$ and $J_4$, the active power of the SSC is not able to track its reference value as can be seen in Fig. 3.

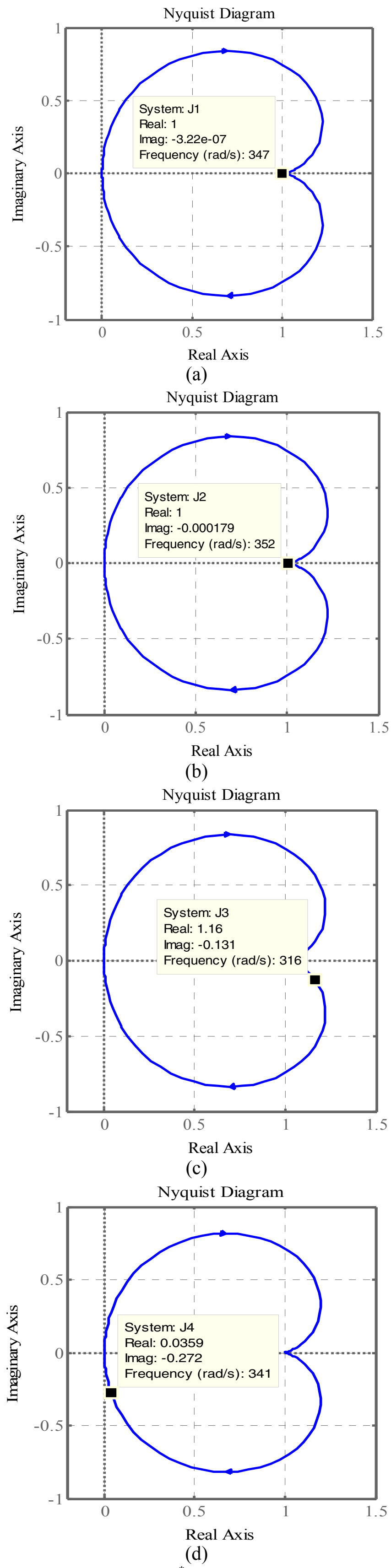


Fig. 3. The Nyquist diagram of $P/P^*$ for different inertia values $J_4>J_3>J_2>J_1$: (a) $J_1$, (b) $J_2$, (c) $J_3$, (d) $J_4$.

The phase and bode diagrams of $P/P^*$ illustrated in Fig. 4, further confirm the aforementioned discussions. Based on this figure, for two first low-value inertias, the phases of this ratio is near to zero around the reference of the angular frequency. However, this is not valid for last two values of $J_3$ and $J_4$. On the other hand, it is apparently seen from (16) that the reactive power component of the SSC is not concerned with SG characteristics.

Fig. 5 and Fig. 6 show the effects of various coefficients of the PI controller on reactive component of the SSC.

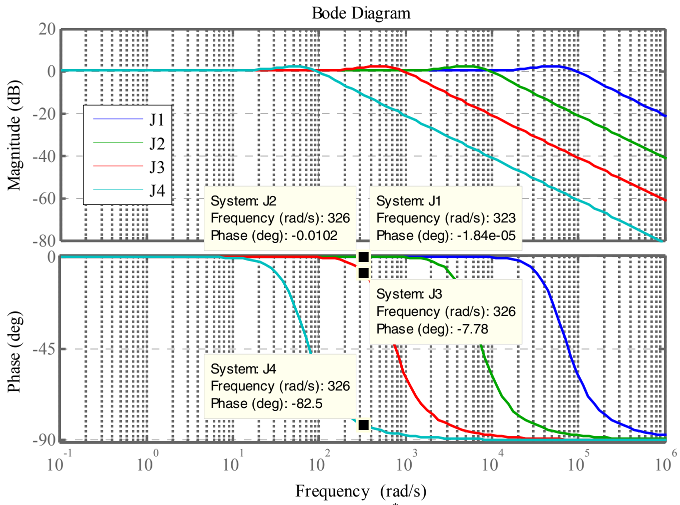


Fig. 4. The phase and bode diagram of $P/P^*$ for various low-value inertias $J_4>J_3>J_2>J_1$.

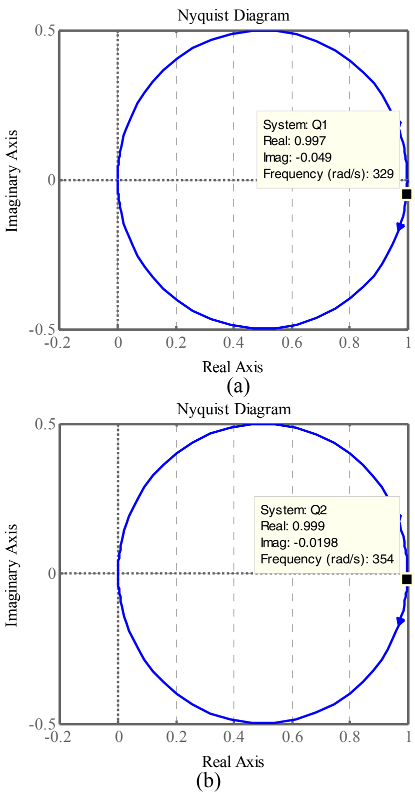


Fig. 5. The Nyquist diagram of $Q/Q^*$ for various coefficients of associated PI controller.

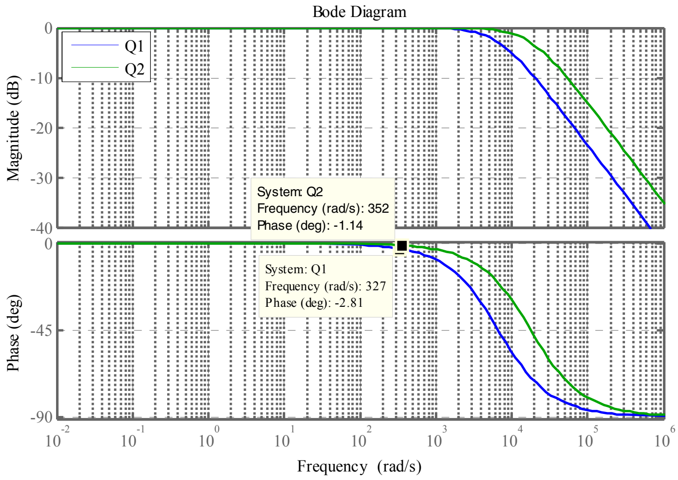


Fig. 6. The phase and bode diagrams of $Q/Q^*$ for various coefficients of associated PI controller.

According to Fig. 5, increasing these coefficients leads to the improvement of the reactive power sharing in the proposed controller as $Q/Q^*$ gets closer to the unit value. The phase diagrams confirm the improvement process as depicted in Fig. 6.

## IV. RESULTS AND DISCUSSIONS

The proposed model in Fig. 7 has been simulated in Matlab/Simulink environment and performance of the SSC is evaluated under different operating conditions. Simultaneous changes of low-value inertia and virtual mechanical power error are considered to ensure the dynamic stability of the SSC under load changes and inversed power flow. The system parameters can be found in Table I.

TABLE I
SIMULATION PARAMETERS

| Parameter | Value | Parameter | Value |
|---|---|---|---|
| dc-link Voltage ($v_{dc}$) | 850 V | $J_1$ | 8e-8 s |
| Phase ac voltage | 220 V | Pm | 3888.9 W |
| Fundamental frequency | 50 Hz | P | 3.5 kW |
| Switching frequency | 10 kHz | Q | 2.5 kVAR |
| REIC resistance | 0.1 Ω | REIC inductance | 45 mH |

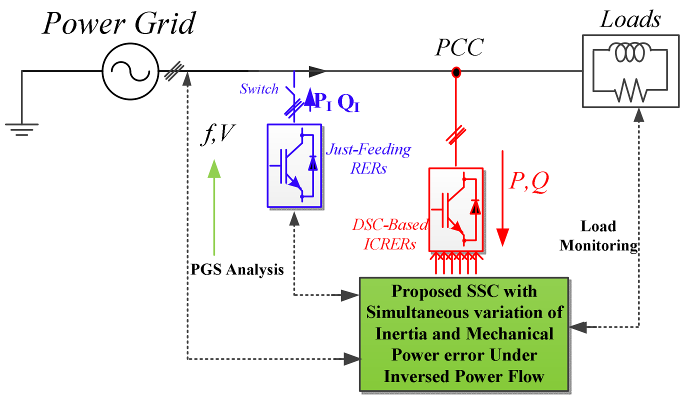


Fig. 7. General structure of the proposed model with simultaneous variation of inertia and VMP error.

The dynamic evaluation of the SSC under a disconnection of RER penetration is discussed in this sub-section. A disconnection of RER power of 4.5kW+j2.5kVar is occurred in the PCC at t=0.1s. Then, after this condition, the SSC-based REIC and PMSG start to provide active and reactive power needed for power grid stability at t=0.25s. Fig. 8 illustrates the active and reactive power of SSC-based RER, voltage magnitude and frequency of grid with the existence of SSC-based RER under RER penetration disconnection operating condition. In this evaluation, the simultaneous changes of low-value inertia and virtual mechanical power error are considered for proposed SSC. The scenario of such a condition is taken into account when the RER penetration disconnection takes place at t=0.1 and the SSC-based RER and PMSG doesn't immediately operate. After experiencing the effects of the disconnection, SSC-based RER and PMSG woks at t=0.25. With the first values of ($\Delta P_{m1}$,$J_1$) shown as blue color, all variable states of SSC-based RER and power grid have their best operation of steady state and dynamic responses as depicted in Fig.8. The worst case is belongs to purple one for ($\Delta P_{m1}$, $J_1$) as shown in Fig.8.

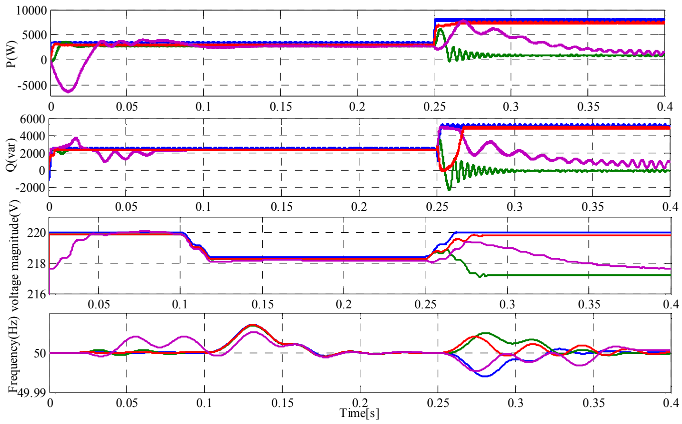


Fig. 8. RER active and reactive power, voltage magnitude and frequency with simultaneous changes of low-value inertia and virtual mechanical power error (($\Delta P_{m4}$, $J_4$)>($\Delta P_{m3}$, $J_3$)>($\Delta P_{m2}$, $J_2$)> ($\Delta P_{m1}$, $J_1$)) during load changes.

## V. CONCLUSION

A single synchronous controller (SSC) has been proposed in this paper for the control of interfaced converters for integration of large-scale renewable energy resources (RERs) into the power grid. All the features of a SG i.e., inertia and virtual mechanical power (VMP) error are considered in the structure of the SSC in order to simulate the behavior of SG in the operation of interfaced converters and provide a stable operation for the power grid under high penetration of RER. An active and reactive power-based dynamic model has been developed and, based on it, two closed-loop control diagrams were shaped in order to analyze the stability of the power grid under different values of characteristics of SG, employed in the SSC. The presented results confirmed that by application of the proposed SSC, the power grid can operate in a stable operating condition under the penetration of large-scale RERs through the power electronic converters.

## REFERENCES


[1] E. Pouresmaeil, M. Mehrasa, M.A. Shokridehaki, E.M.G. Rodrigues, and J.P.S. Catalão, "Control and stability analysis of interfaced converter in distributed generation technology" EUROCON 2015, pp. 1-6, Nov. 2015.

[2] E. Pouresmaeil, M. Mehrasa, and J.P.S. Catalão, "Control strategy for the stable operation of multilevel converter topologies in DG technology," Power Systems Computation Conference (PSCC2014), https://doi.org/10.1109/PSCC.2014.7038494.

[3] M. Mehrasa, M. Rezanejhad, E. Pouresmaeil, JPS Catalao and S. Zabihi, "Analysis and Control of Single-Phase Converter for Integration of Small-Scaled Renewable Energy Sources into the Power Grid," PEDSTC 2016, pp. 384-389, Feb. 2016.

[4] E. Alegria, T. Brown, E. Minear, and R. H. Lasseter, "CERTS microgrid demonstration with large-scale energy storage and renewable generation," IEEE Trans. Smart Grid, vol. 5, no. 2, pp. 937–943, Mar. 2014.

[5] P. Harsha and M. Dahleh, "Optimal management and sizing of energy storage under dynamic pricing for the efficient integration of renewable energy," IEEE Trans. Power Syst., vol. 30, no. 3, pp. 1164–1181, May 2015.

[6] S. Liu, X. Wang, and P. X. Liu, "A Stochastic Stability Enhancement Method of Grid-Connected Distributed Energy Storage Systems," IEEE Trans. Smart Grid, DOI: 10.1109/TSG.2015.2514286. 2017.

[7] T. Stetz, F. Marten, and M. Braun, "Improved low voltage grid-integration of photovoltaic systems in Germany," IEEE Trans. Sustain Energy, vol. 4, no. 2, pp. 534 - 542, June. 2012.

[8] A. Yazdani, A. Di Fazio, H. Ghoddami, M. Russo, M. Kazerani, J. Jatskevich, K. Strunz, S. Leva, and J. Martinez, "Modeling guidelines and a benchmark for power system simulation studies of three-phase single-stage photovoltaic systems," IEEE Trans. Power Del., vol. 26, no. 2, pp. 1247–1264, Apr. 2011.

[9] A. Samadi, R. Eriksson, L. Söder, B. G. Rawn, and J.C. Boemer, "Coordinated Active Power-Dependent Voltage Regulation in Distribution Grids With PV Systems," IEEE Trans. Power Del., vol. 29, no. 3, pp. 1454–1464, Jun. 2014.

[10] E. Pouresmaeil, M. Mehrasa, R. Godina, I. Vechiu, R. L. Rodriguez, and J.P.S. Catalão, "Double Synchronous Controller for Integration of Large-Scale Renewable Energy Sources into a Low-Inertia Power Grid" ISGT, pp. 1-6, Sep. 2017.

[11] M. Mehrasa, R. Godina, E. Pouresmaeil, I. Vechiu, R. L. Rodriguez, and J.P.S. Catalão, "Synchronous Active Proportional Resonant-Based Control Technique for High Penetration of Distributed Generation Units into Power Grids" ISGT, pp. 1-6, Sep. 2017.